NASA/TM–20230005376

Damage Tolerance Comparison of IM7/8552 and T1100/3960 Carbon Fiber/Epoxy Sandwich Structure in Support of the Space Launch System Payload Adapter Fitting

A.T. Nettles, W.E. Guin, and J.P. Mavo
Marshall Space Flight Center, Huntsville, Alabama

I.M. Sadowski
Jacobs ESSCA Group, Huntsville, Alabama

National Aeronautics and
Space Administration

Marshall Space Flight Center • Huntsville, Alabama 35812

April 2023

The NASA STI Program…in Profile

Since its founding, NASA has been dedicated to the advancement of aeronautics and space science. The NASA Scientific and Technical Information (STI) Program Office plays a key part in helping NASA maintain this important role.

The NASA STI Program Office is operated by Langley Research Center, the lead center for NASA's scientific and technical information. The NASA STI Program Office provides access to the NASA STI Database, the largest collection of aeronautical and space science STI in the world. The Program Office is also NASA's institutional mechanism for disseminating the results of its research and development activities. These results are published by NASA in the NASA STI Report Series, which includes the following report types:

- TECHNICAL PUBLICATION. Reports of completed research or a major significant phase of research that present the results of NASA programs and include extensive data or theoretical analysis. Includes compilations of significant scientific and technical data and information deemed to be of continuing reference value. NASA's counterpart of peer-reviewed formal professional papers but has less stringent limitations on manuscript length and extent of graphic presentations.

- TECHNICAL MEMORANDUM. Scientific and technical findings that are preliminary or of specialized interest, e.g., quick release reports, working papers, and bibliographies that contain minimal annotation. Does not contain extensive analysis.

- CONTRACTOR REPORT. Scientific and technical findings by NASA-sponsored contractors and grantees.

- CONFERENCE PUBLICATION. Collected papers from scientific and technical conferences, symposia, seminars, or other meetings sponsored or cosponsored by NASA.

- SPECIAL PUBLICATION. Scientific, technical, or historical information from NASA programs, projects, and mission, often concerned with subjects having substantial public interest.

- TECHNICAL TRANSLATION. English-language translations of foreign scientific and technical material pertinent to NASA's mission.

Specialized services that complement the STI Program Office's diverse offerings include creating custom thesauri, building customized databases, organizing and publishing research results…even providing videos.

For more information about the NASA STI Program Office, see the following:

- Access the NASA STI program home page at <http://www.sti.nasa.gov>

- E-mail your question via the Internet to <help@sti.nasa.gov>

- Phone the NASA STI Help Desk at 757–864–9658

- Write to:
  NASA STI Information Desk
  Mail Stop 148
  NASA Langley Research Center
  Hampton, VA 23681–2199, USA

NASA/TM–20230005376

Damage Tolerance Comparison of IM7/8552 and T1100/3960 Carbon Fiber/Epoxy Sandwich Structure in Support of the Space Launch System Payload Adapter Fitting

A.T. Nettles, W.E. Guin, and J.P. Mavo
Marshall Space Flight Center, Huntsville, Alabama

I.M. Sadowski
Jacobs ESSCA Group, Huntsville, Alabama

National Aeronautics and
Space Administration

Marshall Space Flight Center • Huntsville, Alabama 35812

April 2023

TRADEMARKS

Trade names and trademarks are used in this report for identification only. This usage does not constitute an official endorsement, either expressed or implied, by the National Aeronautics and Space Administration.

Available from:

NASA STI Information Desk
Mail Stop 148
NASA Langley Research Center
Hampton, VA 23681–2199, USA
757–864–9658

This report is also available in electronic form at
<http://www.sti.nasa.gov>

TABLE OF CONTENTS

LIST OF FIGURES

LIST OF TABLES

LIST OF ACRONYMS, ABBREVIATIONS, AND SYMBOLS

ASTM	American Society for Testing and Materials
ATL	automatic tape laying
CAI	compression after impact
CMA	Composite Materials America
ft·lb	foot-pound
MSFC	Marshall Space Flight Center
NDE	nondestructive evaluation
PAF	Payload Adapter Fitting
SLS	Space Launch System
S	symmetric
t_{max}	maximum thickness
t_{min}	minimum thickness

TECHNICAL MEMORANDUM

DAMAGE TOLERANCE COMPARISON OF IM7/8552 AND T1100/3960 CARBON FIBER/ EPOXY SANDWICH STRUCTURE IN SUPPORT OF THE SPACE LAUNCH SYSTEM PAYLOAD ADAPTER FITTING

1. INTRODUCTION

As technology evolves and improves within the science of composite materials, new fiber/resin systems are being developed for improved properties given certain loading and environmental scenarios. Improving the room temperature damage tolerance capabilities has long been one of the goals in the carbon fiber/polymer composite industry. Recently a new fiber/epoxy system has been introduced that is claimed to have superior damage tolerance capabilities. To examine if this new carbon fiber/epoxy composite material would be of benefit to a program to manufacture a Payload Adapter Fitting (PAF) for NASA's Space Launch System (SLS) rocket, the question was asked as to just how much damage tolerance could be realized if this new system were used.

Compression after impact (CAI) strength of sandwich structure is one of the leading metrics being used to evaluate materials for the PAF program. As a result, a comparison of this new fiber/resin system with a very common (and planned baseline) fiber/resin system with respect to CAI was considered in this study. While it was already known that the older, baseline carbon fiber structure would not have as good damage tolerance characteristics as the newer carbon fiber system, the quantitative difference in damage tolerance was sought in this study since no other CAI data could be found in open literature on sandwich structures made with this new fiber/resin system.

2. MATERIALS AND TESTING

2.1 Materials

The two carbon/epoxy face sheet materials used in this study were Hexcel® HexTow®/ HexPly® IM7/8552 and Toray Composite Materials America (CMA) TORAYCA™ T1100/3960. Table 1 shows some of the properties of these two fiber/resin systems using data supplied by the vendors.

Table 1. Some key composite properties of the two fiber/resin systems used in this study.

Composite Property	Hexcel IM7/8552[1,2]	Toray CMA T1100/3960[3,4]
0° Tensile Strength	395 ksi	572 ksi
0° Tensile Modulus	23.8 Msi	25.3 Msi
0° Compressive Strength	245 ksi	297 ksi
0° Compressive Modulus	21.7 Msi	22.2 Msi
CAI	34 ksi	48.7 ksi
0° Short Beam Shear	19.9 ksi	16.5 ksi
Open Hole Compressive Strength	48.9 ksi	48.8 ksi
Fiber Strain to Failure	1.8%	2.0%
Fiber Volume fraction	60%	60%

Of note in the above table, the CAI value (i.e., impact energy of 1,500 in·lb/in, per American Society for Testing and Materials (ASTM) standard D7137) of the newer Toray fiber/resin system is 43% higher. It will be of interest to see if this large difference is realized using thinner laminates in the form of face sheets on honeycomb sandwich structure. The open hole compression strength, which can be a good predictor of CAI strength for a given damage size, is about the same for the two fiber/resin systems. Thus, the higher CAI strength of the newer system should be due to a smaller damage size being formed for a given impact energy.

The sandwich structure used in this study was manufactured by co-curing the face sheets to aluminum honeycomb core. The core had a density of 4.5 lb/ft^3. All the face sheets were manufactured by automatic tape laying (ATL) at NASA Marshall Space Flight Center (MSFC). The IM7/8552 tape had an areal weight of 190 g/m^2 and the T1100/3960 tape also had an areal weight of 190 g/m^2. The honeycomb sandwich structure was manufactured with the core ribbon, or 'L' direction aligning with the 0° fiber direction. The 8-ply face sheets had a symmetric (S) lay-up of [–45/90/+45/0]S. The sandwich structure had a layer of Solvay FM® 300-2M epoxy film adhesive placed over the core material prior to the ATL process used to manufacture the face sheets.

The sandwich structure was cured in an autoclave at 350 °F with a pressure of 40 psi. The flat sandwich panels made for use in this study measured 36 × 36 in. The sandwich structure

showed good consolidation with some porosity, mostly in the IM7/8552 material as shown in figure 1. Typical fiber waviness of the face sheets (i.e., the inner plies closest to the honeycomb core panels) was noted. The thickness values of the face sheets on the honeycomb panels varied from a minimum at the cell walls (t_{min}) to a maximum between the cell walls (t_{max}) as shown in the top cross-sectional photomicrograph in figure 1. A nominal value for the face sheet thickness can be found based on the average of numerous random thickness measurements.

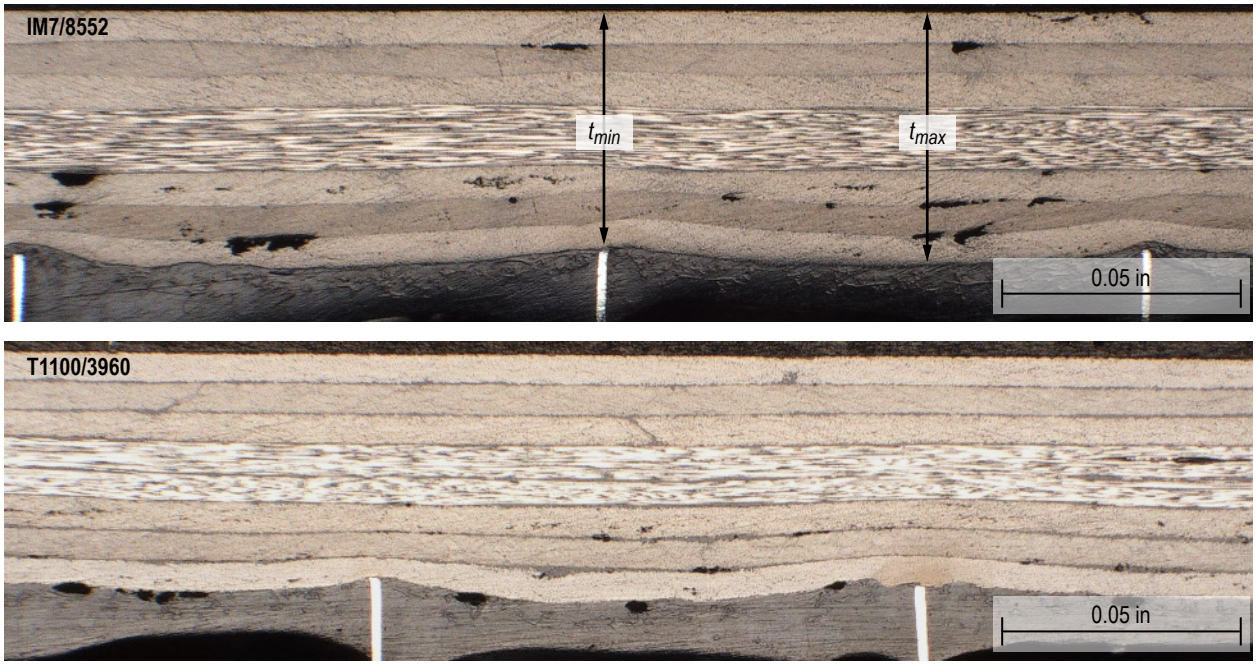

Figure 1. Cross-sectional photomicrographs showing face sheet waviness of inner plies on honeycomb core specimen for both fiber/resin face sheets used in this study.

Using photomicroscopy and measuring tools contained within the software attached to the microscope, the nominal face sheet thicknesses of the specimens tested was measured and was found to be 0.050 in for both the IM7/8552 and T1100/3960 fiber/resin face sheets. The large sandwich panel was cut into 6-in-tall (direction of loading) by 4-in-wide specimens using a diamond saw. The specimens were cut such that the loading direction was parallel to the core ribbon, or 'w' direction, thus giving a face sheet lay-up of [+45/0/–45/90]S. This orientation has been shown to be the most vulnerable to impact damage[5] and was chosen for this reason. The top and bottom edges of these specimens were then machined to ±0.001-in tolerance of parallelism using a vertical end mill with a solid carbide cutting tool (LMT Onsrud 67–526 designed for carbon fiber machining). The side edges of the specimens were machined to be perpendicular to the top and bottom edges.

Undamaged strength testing of the honeycomb sandwich structure was not pursued in this study since the undamaged specimens exhibited end-brooming which is not a valid failure mode, and this study concerns damage tolerance testing and undamaged strength values are not relevant. The modulus for each of the two types of sandwich structure was measured and found to be 8.7 Msi for the IM7/8552 sandwich structure and 9.5 Msi for the T1100/3960 sandwich structure.

2.2 Impact Damage Testing

Each sandwich specimen was impacted at its geometric center on the tool side face sheet since the tool side is to be the outer side of the PAF structure and thus the most prone to impact damage. A caul plate was used on the bag side of the sandwich panel during fabrication and thus there was essentially no difference between the two face sheets. The impactor had a diameter of 0.5 in and each specimen was placed on a solid steel plate during impact to give the highest rigidity, and thus most damage possible for a given impact energy.[6,7] This also ensured similar boundary conditions for all impacts. An instrumented drop weight impact apparatus was used to inflict damage to the specimens. A picture of the impact tester used is shown in figure 2. The selected impact energies, measured in foot-pounds (ft·lb), were based on what was determined to be easily visible impact damage for the IM7/8552 sandwich specimens tested (5.6 ft·lb). An impact energy less than this and three larger than this were chosen for the remainder of impacts on the sandwich specimens so that residual strength curves could be constructed. Results of the impact tests showing the impact energy used, number of specimens tested, the dent depth formed and the maximum load of impact on the specimens are summarized in table 2. The dent measurements were taken at least 24 hours after impact to allow for any reduction or 'relaxation' of the dent depth. The maximum load of impact is the largest load recorded during the impact event.

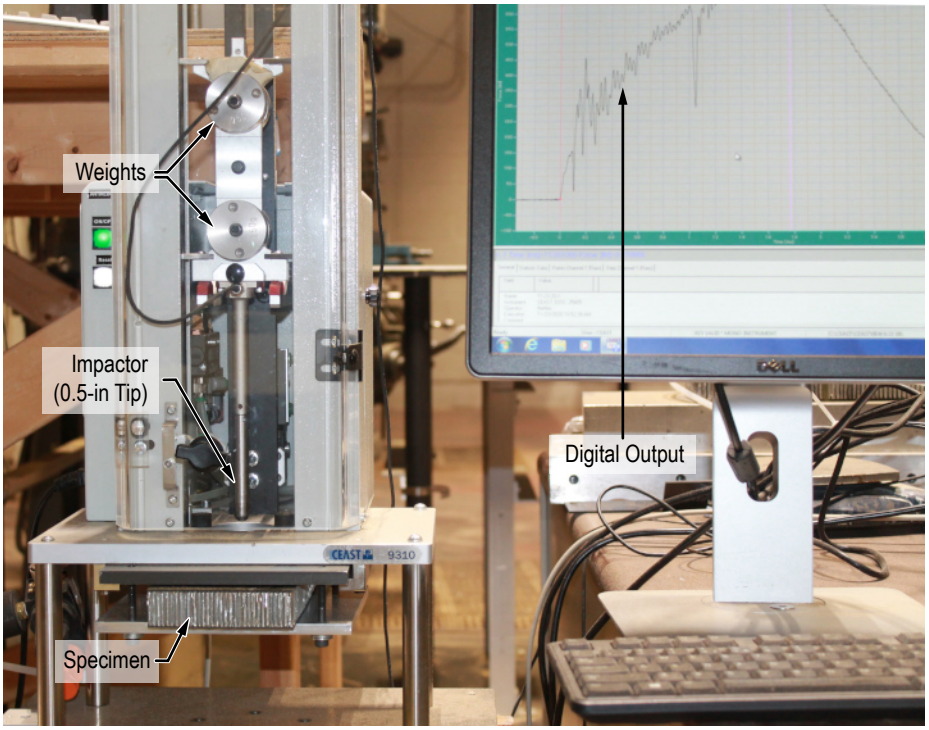

Figure 2. Photograph of instrumented impactor used in this study.

Table 2. Summary of results from impact testing on sandwich specimens used in this study.

Face Sheet	Impact Energy (ft·lb)	Specimens Tested	Dent Depth (mil)	Maximum Impact Load (lb)
IM7/8552	2.8	4	14 ± 3	614 ± 7
	5.6	4	41 ± 4	784 ± 17
	8.0	5	60 ± 6	766 ± 16
	10.5	4	69 ± 8	785 ± 30
	13.2	3	127 ± 23	788 ± 54
T1100/3960	2.8	3	18 ± 2	644 ± 28
	5.6	5	28 ± 2	949 ± 17
	8.0	6	40 ± 4	1096 ± 22
	10.5	5	70 ± 5	1156 ± 67
	13.2	4	85 ± 8	1157 ± 78

Figure 3 shows plots of the data in table 2. The dent depth appears to increase linearly with increasing impact energy with the T1100/3960 data showing a slightly smaller dent depth for most of the impact energies. The maximum load of impact data shows that the IM7/8552 specimens quickly reach an ultimate maximum load of impact (basically face sheet penetration) of about 800 lb while the T1100/3960 specimens do not reach the ultimate maximum (i.e.,face sheet penetration) load until the highest impact energy level was used. Thus, the T1100/3960 specimens are much more damage resistant. Compression testing of these specimens will reveal their tolerance to these damage states.

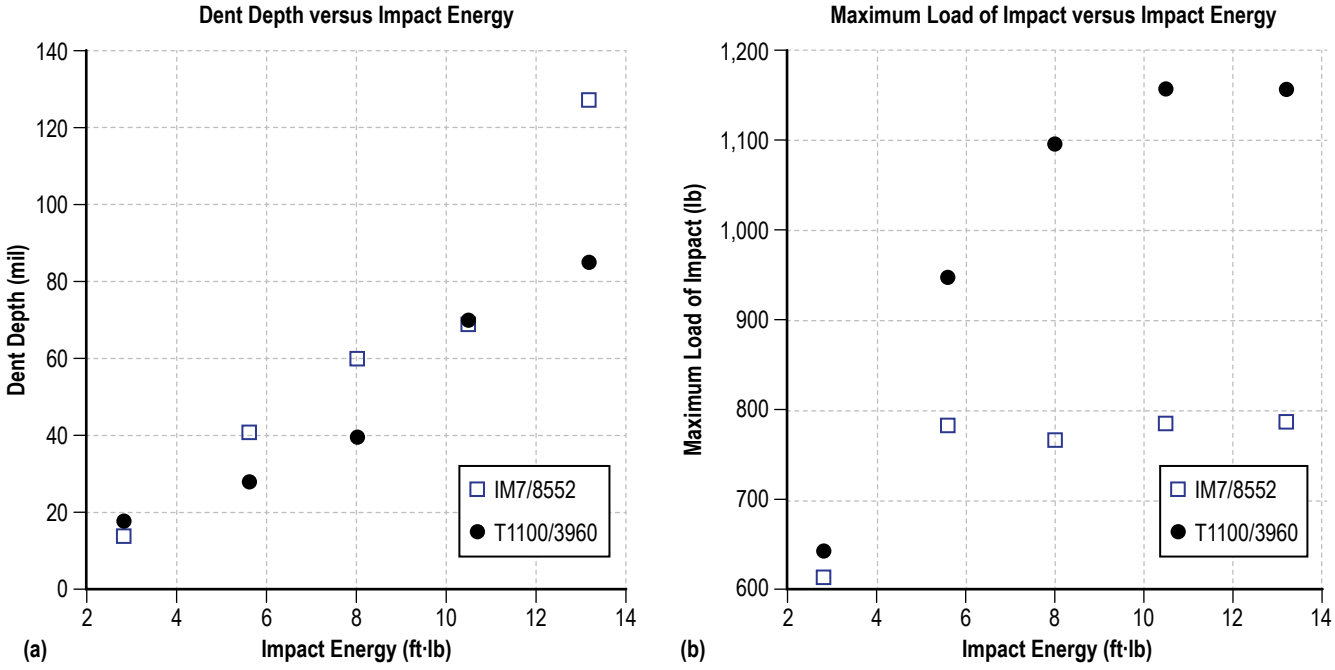

Figure 3. Plots of (a) dent depth versus impact energy and (b) maximum load of impact versus impact energy from Table 1.

Samples of visual damage on the impacted specimens produced by each of the various levels of impact energy are shown in figure 4. It should be noted that in practice, the amount of visual damage in the field will vary depending upon such factors as the available lighting, the angle of the lighting, and the surface finish of the specimen. All the impacts can be visually detected, which will be beneficial in practice since even low energy impacts will be noted and can be dispositioned.

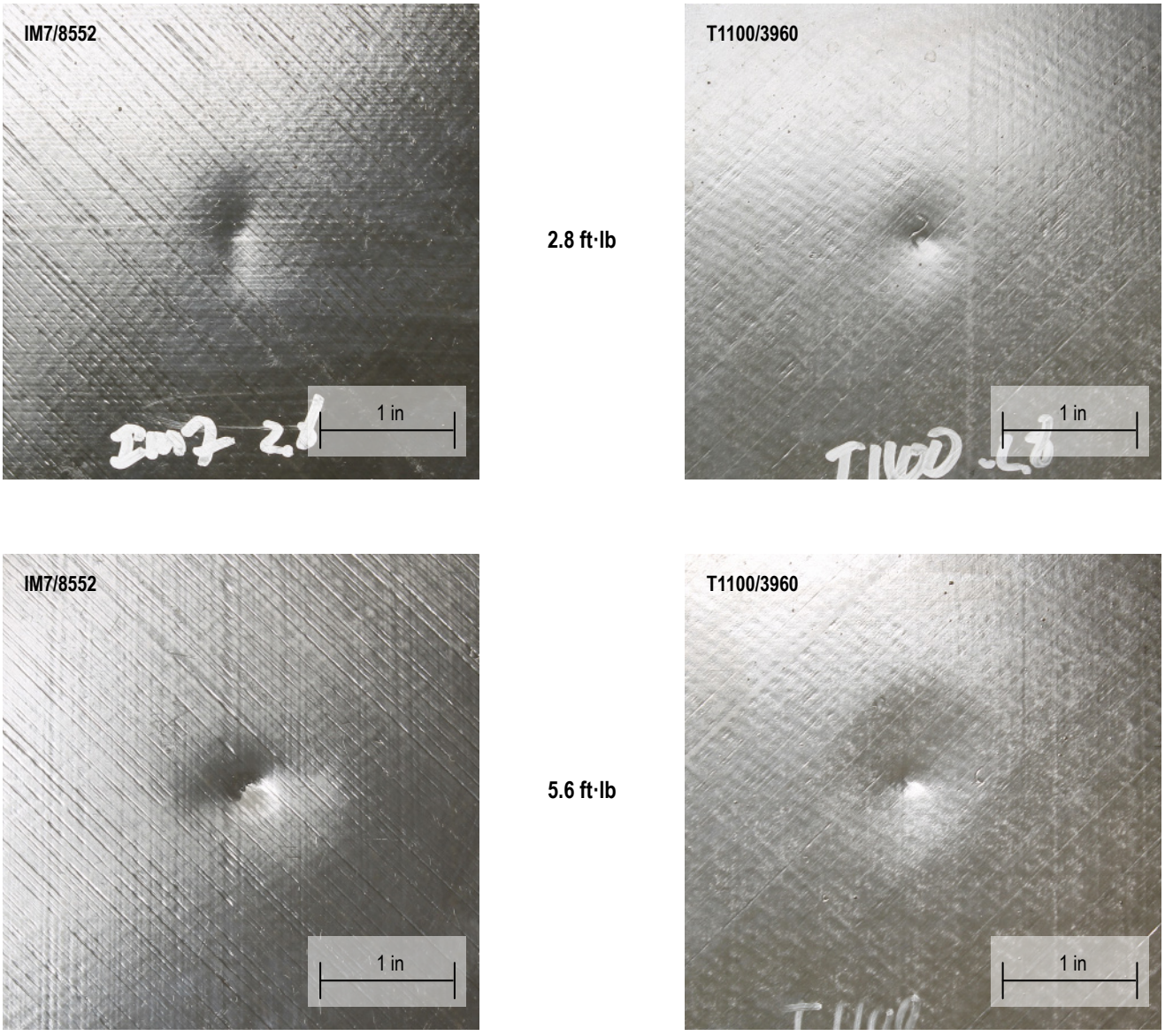

Figure 4. Photographs of various impacts with a 0.5-in impactor on honeycomb core sandwich structure with IM7/8552 and T1100/3960 face sheets.

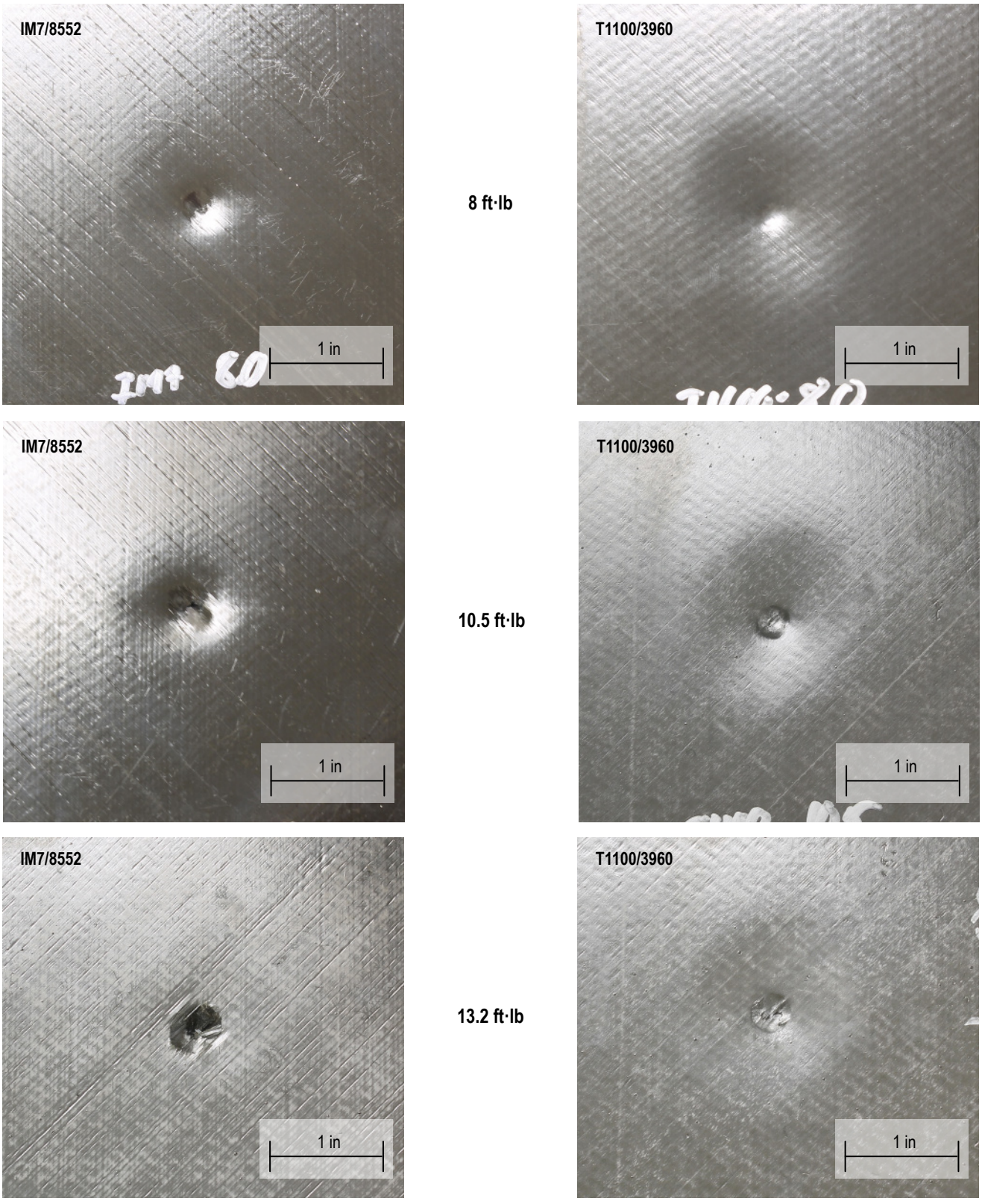

Figure 4. Photographs of various impacts with a 0.5-in impactor on honeycomb core sandwich structure with IM7/8552 and T1100/3960 face sheets.

Sample load-deflection data from each level of impact event are shown in figure 5.

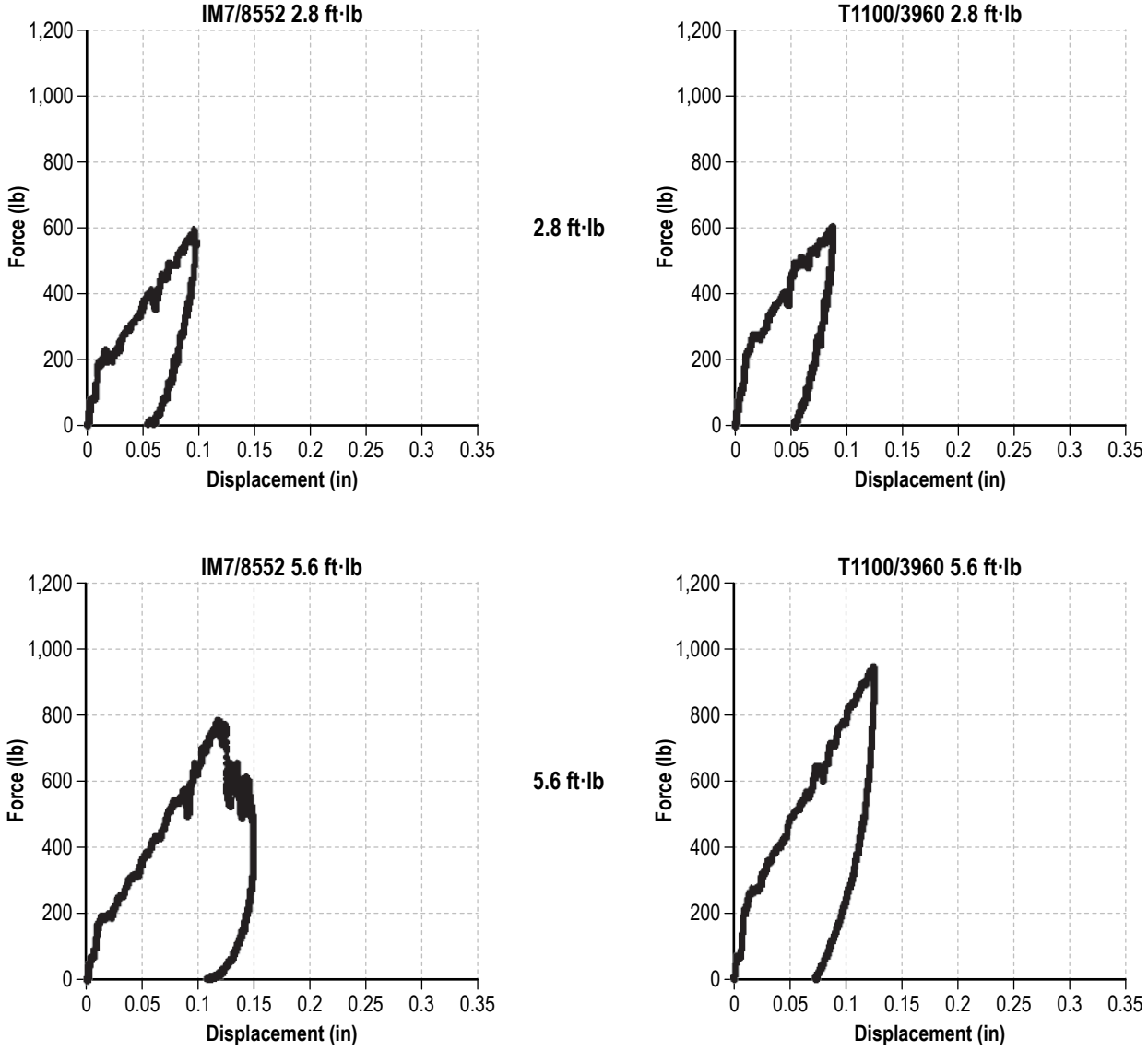

Figure 5. Load-deflection data of various impacts on honeycomb core specimens used in this study.

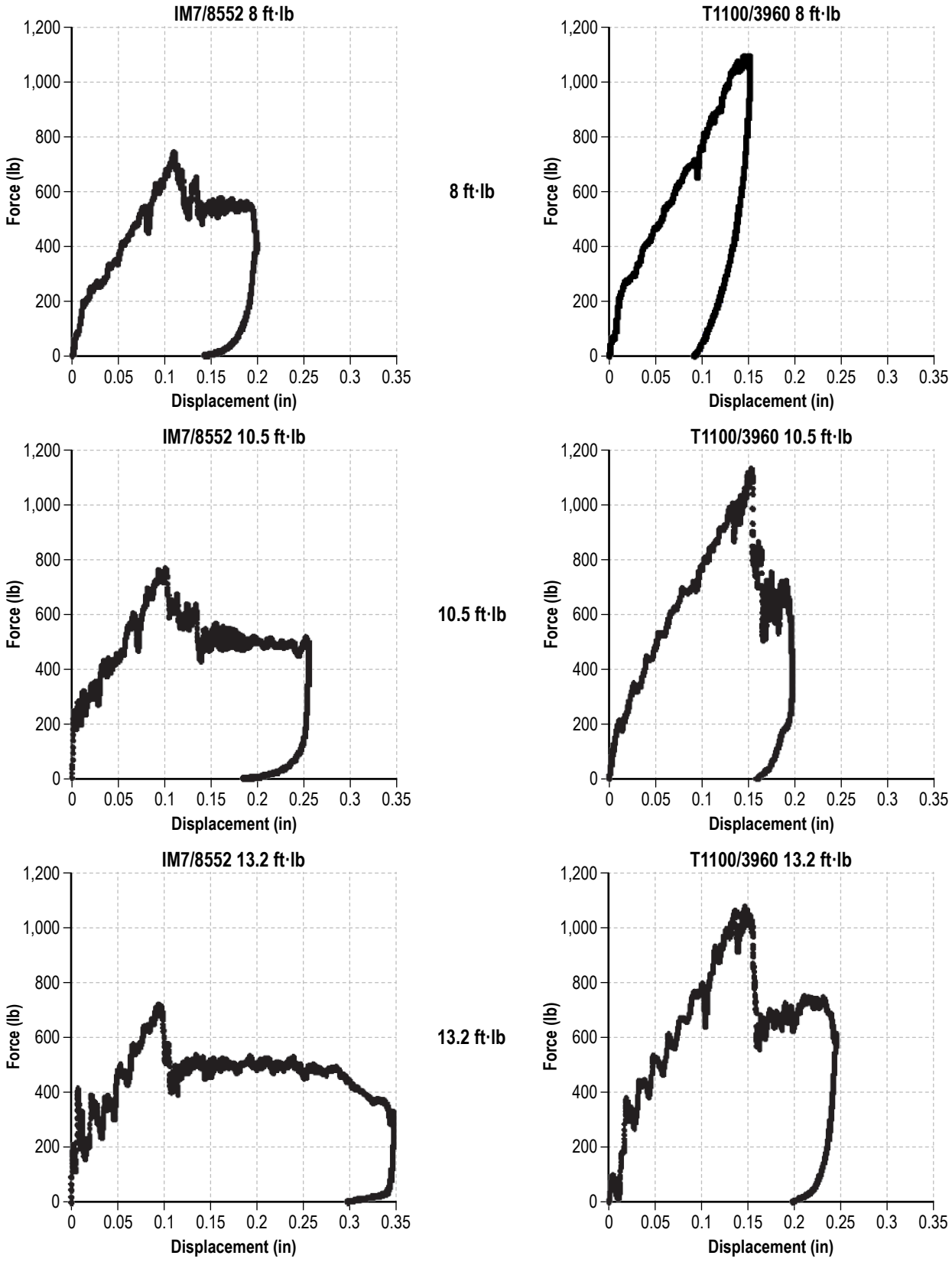

Figure 5. Load-deflection data of various impacts on honeycomb core specimens used in this study.

For the lowest impact energy tested, the two types of specimens have nearly identical load-deflection curves, but the IM7/8552 specimens show more energy being absorbed (area under the curve) for a given impact energy as the impact energy increases than the T1100/3960 specimens indicating less damage resistance as was also determined from the maximum impact load data (right side of figure 3).

Nondestructive evaluation (NDE) in the form of flash thermography was performed on the impacted specimens and samples from each face sheet at each of the impact energy levels are presented in figure 6. The so-called 'damage size' is the diameter of a circle circumscribed around the damage indication as shown in the first two thermography images.

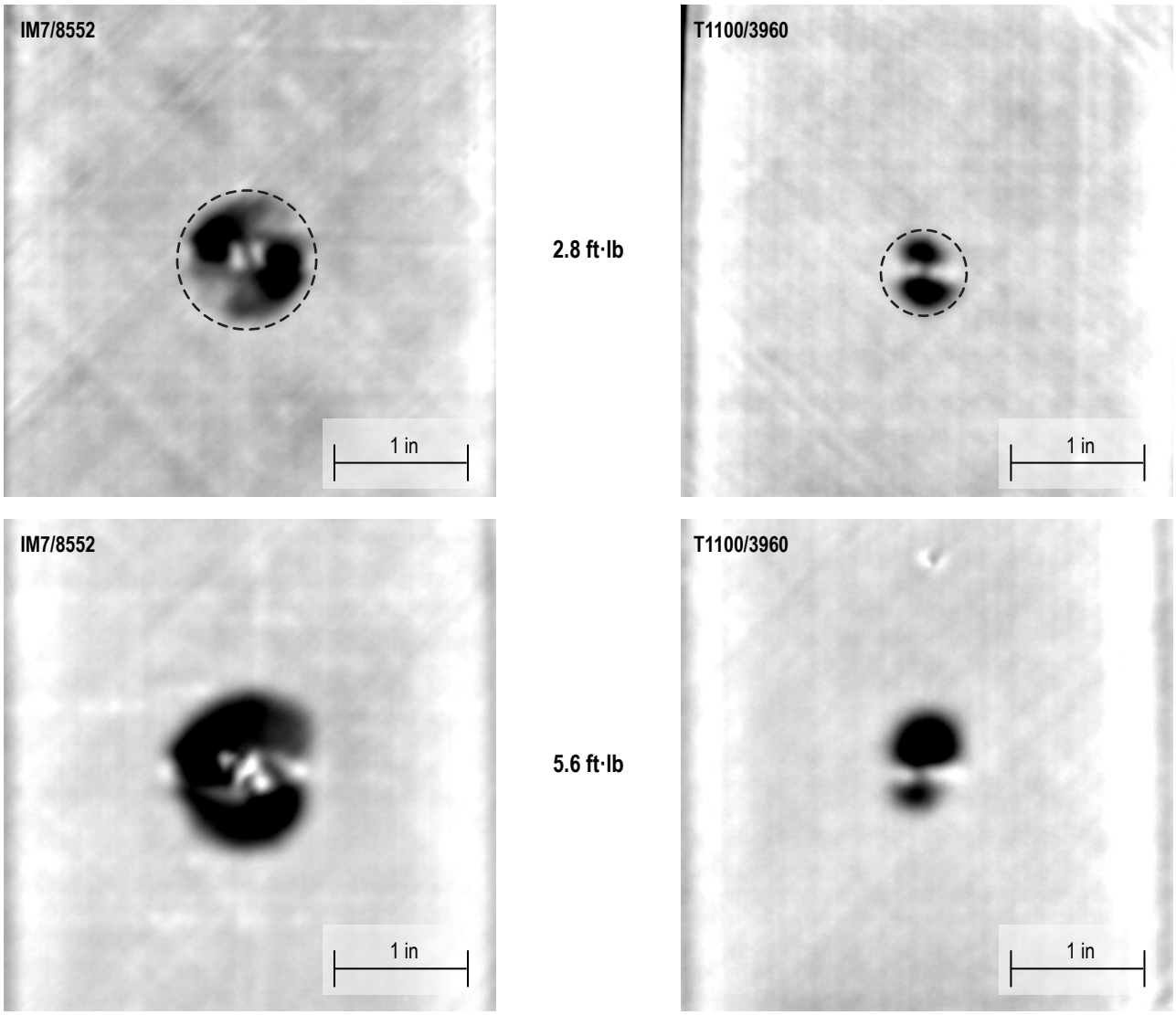

Figure 6. Thermography signatures of various impacts on honeycomb core specimens used in this study.

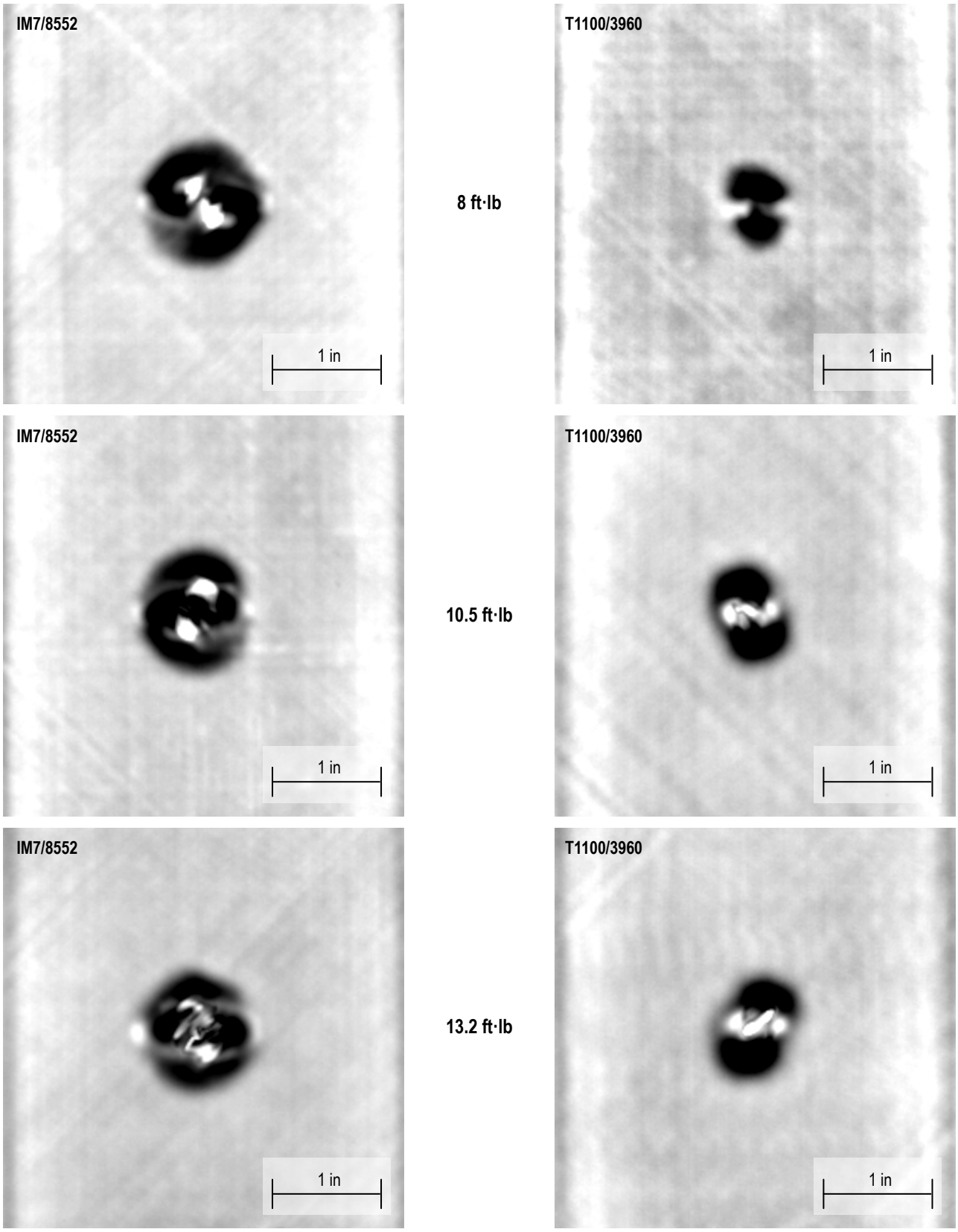

Figure 6. Thermography signatures of various impacts on honeycomb core specimens used in this study.

The size of the damage is consistently larger for the IM7/8552 face sheet sandwich structures at any given impact severity level. Quantitative data for the damage size (as determined by the diameter of the circular indications seen in the thermography images is given in table 3 and plotted graphically in figure 7.

Table 3. Summary of thermography results on impacted specimens.

Face Sheet	Impact Energy (ft·lb)	Damage Size (in)
IM7/8552	2.8	0.98 ± 0.04
	5.6	1.23 ± 0.08
	8.0	1.27 ± 0.01
	10.5	1.19 ± 0.21
	13.2	1.19 ± 0.08
T1100/3960	2.8	0.56 ± 0.04
	5.6	0.70 ± 0.05
	8.0	0.70 ± 0.03
	10.5	0.81 ± 0.02
	13.2	0.87 ± 1.00

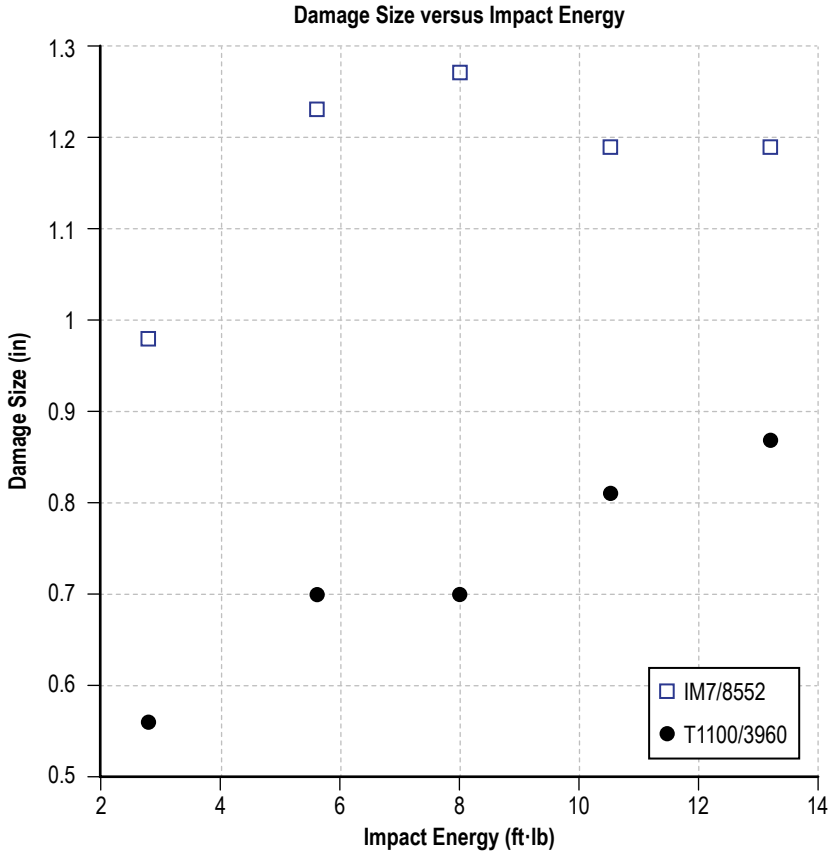

Figure 7. Damage size as determined by thermography versus impact energy.

These data correlate well with what was seen in the maximum load of impact data shown in figure 3, in which the IM7/8552 specimens reached a ‘saturation’ value after the lowest impact energy was reached, indicating a lower damage resistance.

Examples of the through thickness severity of the damage in the face sheets is shown by the cross sections presented in figure 8. These cuts were made through the center of the damage zone in the 90° direction (width direction). The IM7/8552 specimens show more through thickness damage than the T1100/3960 specimens for any given impact energy.

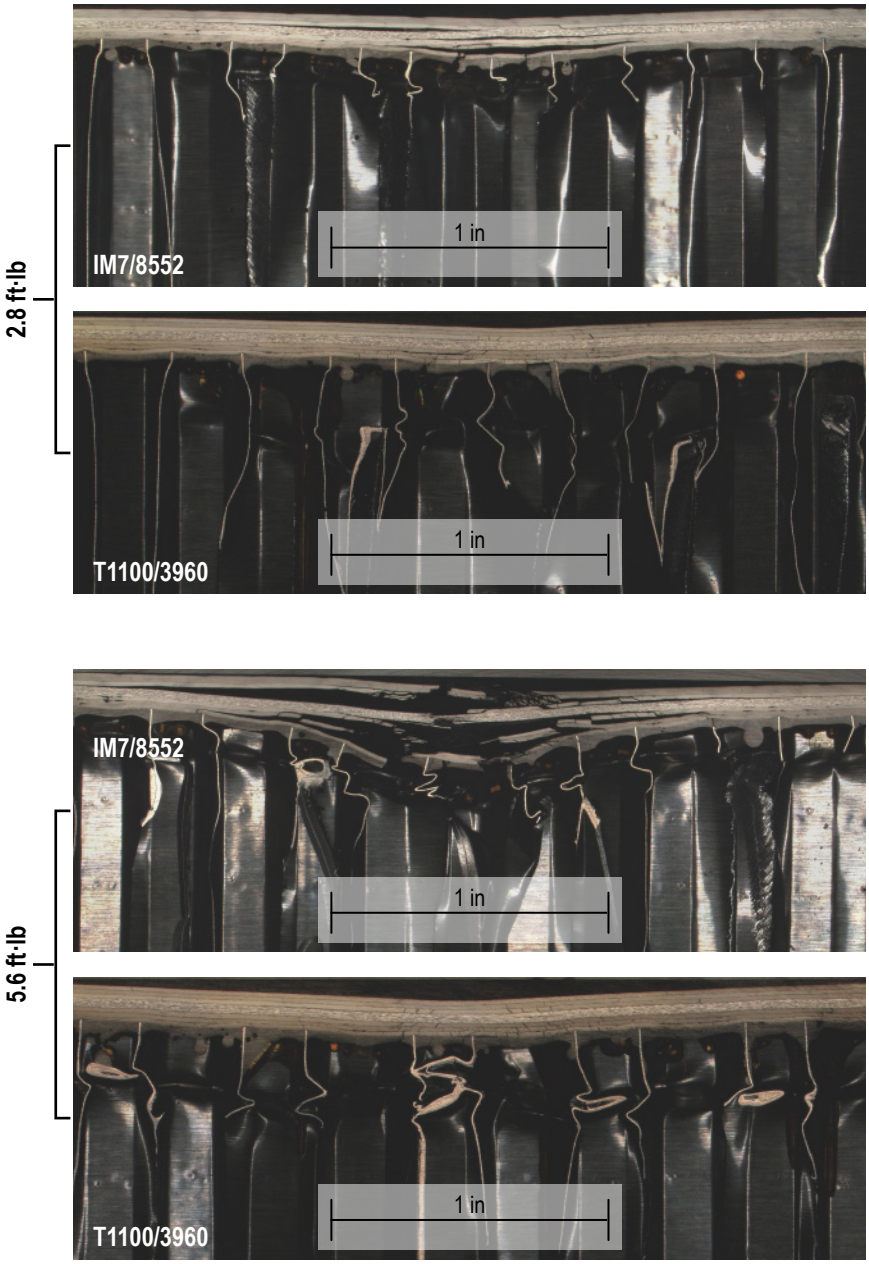

Figure 8. Cross-sectional photomicroscopy of various impacts on honeycomb core specimens used in this study. Cuts made in the 90° direction.

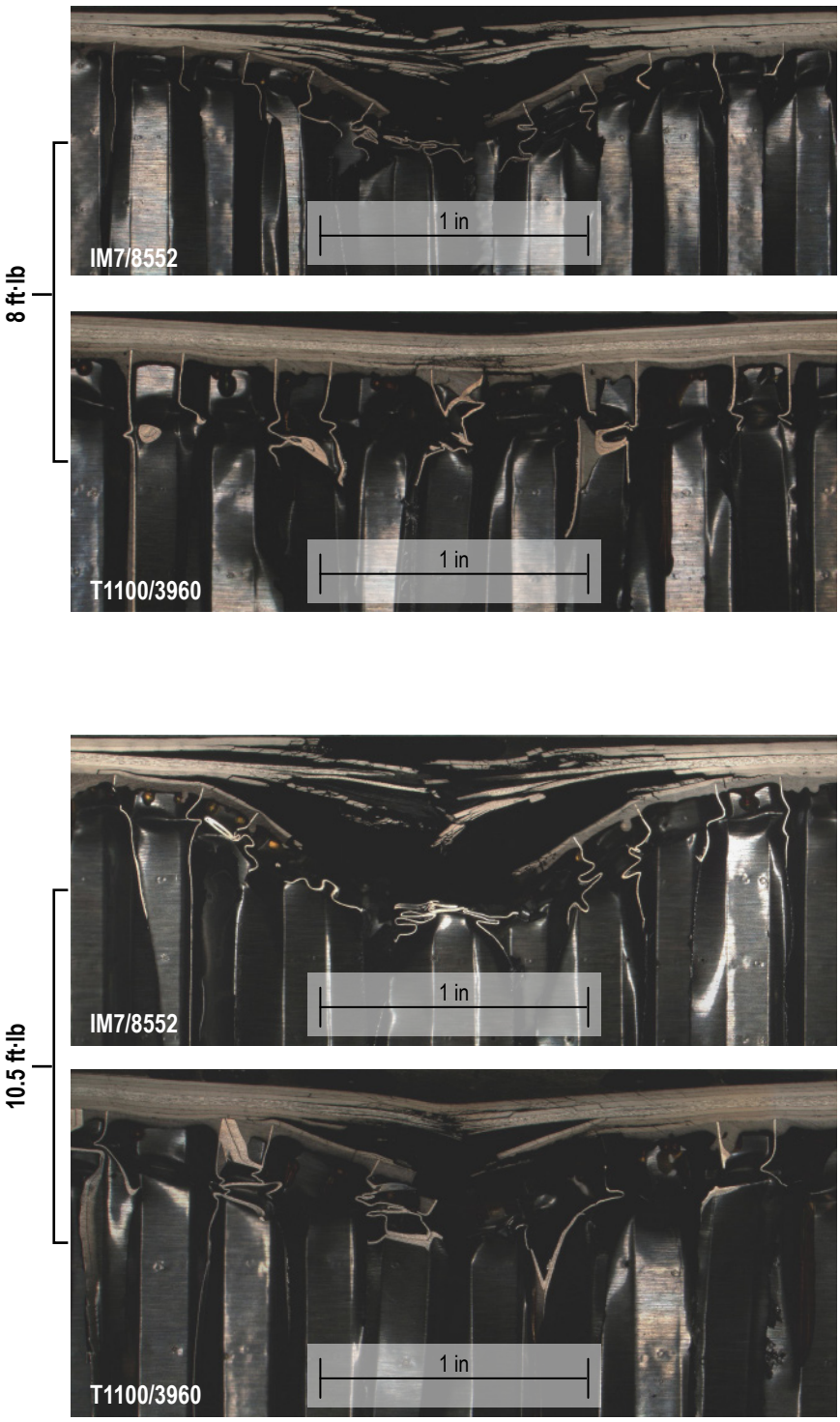

Figure 8. Cross-sectional photomicroscopy of various impacts on honeycomb core specimens used in this study. Cuts made in the 90° direction.

Figure 8. Cross-sectional photomicroscopy of various impacts on honeycomb core specimens used in this study. Cuts made in the 90° direction.

2.3 Compression After Impact Testing

The impacted sandwich specimens were assessed for residual compression strength using the test fixture shown in figure 9. Three strain gages were placed on the specimen as diagramed in figure 10 to ensure even loading of each of the face sheets. The specimens were taken to approximately 1,000 microstrain and if one gage was lower than the others by more than 10%, shims were placed under the edge that was reading low until the gages were even. During compression testing the gages were monitored and if any deviation greater than 10% occurred, the test was stopped. Shims would be rearranged until the gages read within 10% of each other, and then the test would be continued until each specimen failed.

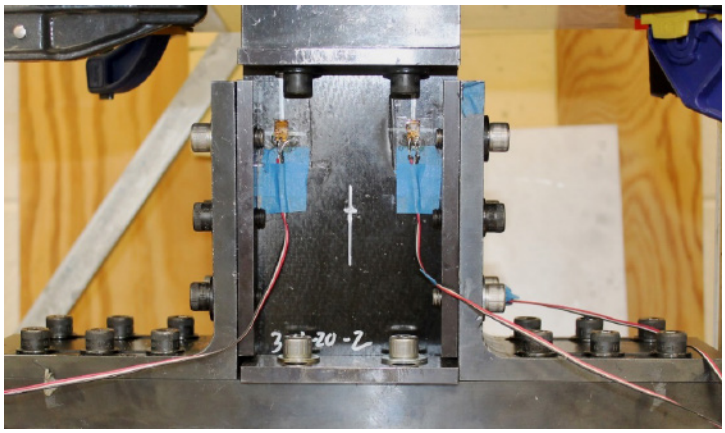

Figure 9. Photograph of fixture used for assessing CAI strength of sandwich specimens.

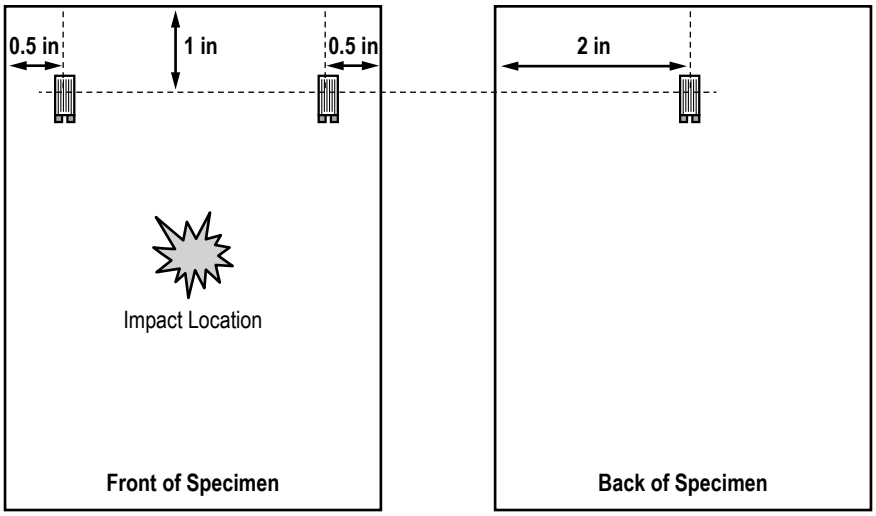

Figure 10. Location of strain gages on front and back of each CAI specimen.

For the specimens impacted at the lowest two impact energies for each of the two types of fibers used, the ends needed to be potted to prevent end brooming. This was accomplished by crushing the core about 0.25-in deep across the top and bottom of the specimen and filling these channels with paste epoxy resin as shown in figure 11. This prevented end brooming.

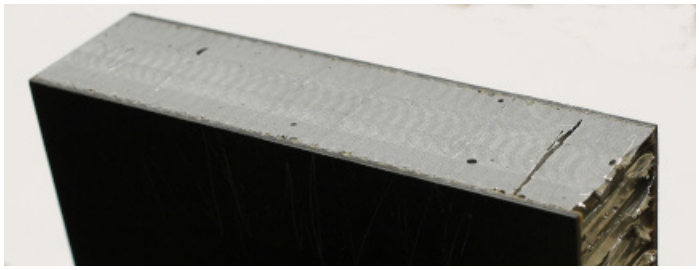

Figure 11. Picture of potted end of CAI specimen.

Typical failures from each type of specimen are shown in figure 12. All failures were through the impact damage and ran perpendicular to the loading direction. The IM7/8552 specimens tended to bulge out more along the failure zone than the T1100/3960 specimens, which tended to show less out-of-plane damage along the failure zone post-testing. This probably is an indicator of the interlaminar fracture toughness being higher for the T1100/3960 face sheet specimens.

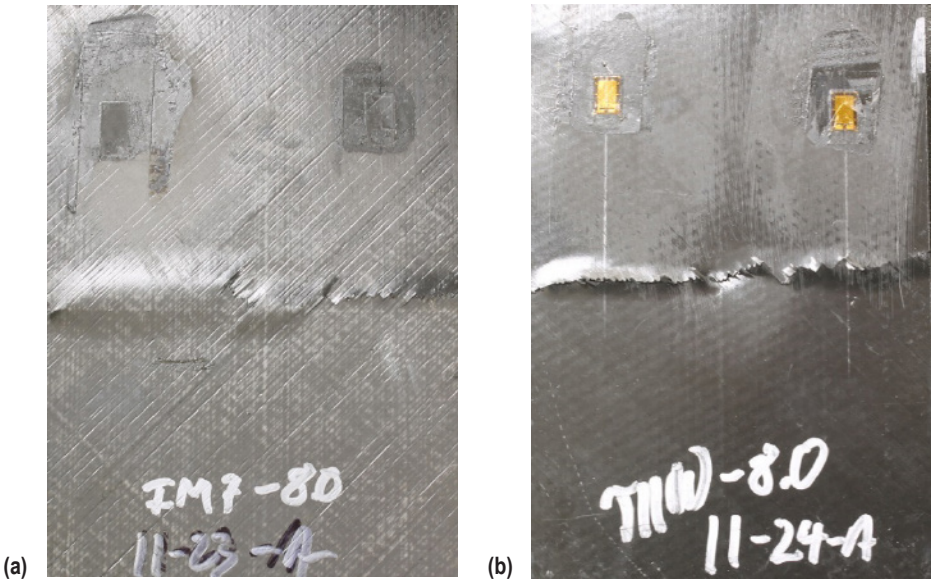

Figure 12. Picture of (a) failed IM7/8552 CAI specimen and (b) failed T1100/3960 CAI specimen.

The CAI strength results are presented in table 4. As the damage level becomes more severe, the difference in CAI strength of the two types of specimens becomes smaller, as can be seen on the impact energy plots in figure 13. However, even at the most severe impact levels used in this study, the T1100/3960 specimens have about a 20% higher CAI strength. At the lower end of impact energies used, the T1100/3960 specimens had approximately 50% higher compression load carrying capability.

Table 4. Summary of CAI results of the sandwich specimens tested in this study.

Face Sheet	Impact Energy (ft·lb)	Specimens Tested	CAI Strength (ksi)
IM7/8552	2.8	4	44.3 ± 1.1
	5.6	4	39.1 ± 1.3
	8.0	5	35.7 ± 4
	10.5	4	35.9 ± 2.2
	13.2	3	35.7 ± 1.4
T1100/3960	2.8	3	67.1 ± 2.5
	5.6	5	60.4 ± 2.4
	8.0	6	52.5 ± 2.3
	10.5	5	41.6 ± 3.1
	13.2	4	42.4 ± 1.8

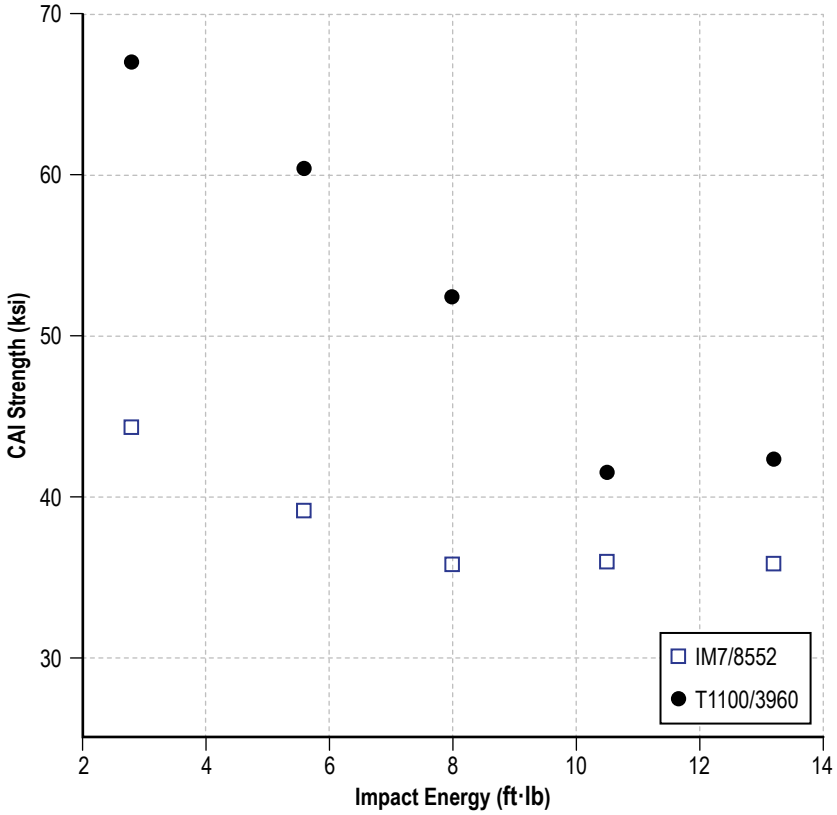

Figure 13. CAI results of IM7/8552 sandwich specimens and T1100/3960 sandwich specimens.

3. CONCLUSIONS

The sandwich specimens with the T1100/3960 face sheets are significantly more damage tolerant than sandwich specimens made with IM7/8552 face sheets to the order of about a 50% increase in CAI strength, except at very high impact severity levels where the T1100/3960 face sheet specimens had about a 20% increase in compressive load carrying capability. From the maximum load of impact data, damage size data and through-thickness damage morphology, it is clear that the T1100/3960 system has better damage resistance.

REFERENCES

1. Hexcel, "HexTow Laminate Properties in HexPly® 8552," https://www.hexcel.com/Products/Resources/1664/hextow-laminate-properties-in-hexply-8552, 2023.

2. Hexcel, "HexTow® IM7 Carbon Fiber Product Data Sheet," https://www.hexcel.com/user_area/content_media/raw/IM7_HexTow_DataSheet.pdf, 2020.

3. Toray Composite Materials America, "3960 Prepreg System Data Sheet," https://www.toray-cma.com/wp-content/uploads/3960-Prepreg-System.pdf, August 9, 2022.

4. Toray Composite Materials America, "T1100G Intermediate Modulus Carbon Fiber," https://www.toraycma.com/wp-content/uploads/T1100G-Technical-Data-Sheet-1.pdf.pdf, January 17, 2018.

5. Nettles, A.T.; Guin, W.E.; and Sadowski, I.: "The Effects of Loading Direction on the Compression After Impact Strength of quasi-isotropic face sheet honeycomb core sandwich structure," *Journal of Sandwich Structures and Materials*, Vol. 24, No. 7, pp. 2013-2029, doi:10.1177/10996362221116572, July 20, 2022.

6. Tomblin, J.S.; Ng, Y.C.; and Raju, K.S.: "Material qualification and equivalency for polymer matrix composite material systems," DOT/FAA/AR-00/47, Office of Aviation Research, Washington, D.C., https://www.tc.faa.gov/its/worldpac/techrpt/ar00-47.pdf, April, 2001.

7. Nettles, A.T.; and Jackson, J.R.: "Developing a material strength design value based on compression after impact (CAI) damage for the ARES I composite interstage," NASA/TP-2009-215634, Marshall Space Flight Center, Huntsville, AL, https://ntrs.nasa.gov/api/citations/20090007473/downloads/20090007473.pdf, January, 2009.

National Aeronautics and
Space Administration
IS02
George C. Marshall Space Flight Center
Huntsville, Alabama 35812